Oxygen 1s x-ray-absorption edges of transition-metal oxides

F. M. F. de Groot, M. Grioni, and J. C. Fuggle
Research Institute for Materials, University of Nijmegen, Toernooiveld, NL-6525 ED Nijmegen, The Netherlands

J. Ghijsen and G. A. Sawatzky
Materials Science Centre, University of Groningen, Paddepoel, Nijenborgh 18, NL-9747 AG Groningen, The Netherlands

H. Petersen
Berliner Elektronenspeicherring-Gesellschaft für Synchrotronstrahlung m.b.H. (BESSY), Lentzeallee 100, D-1000 Berlin 33, Federal Republic of Germany

(Received 17 February 1989; revised manuscript received 8 May 1989)

The oxygen 1s x-ray-absorption edges of a series of 3d-transition-metal oxides have been measured. The structures at the edge arise from covalent mixing of the metal and oxygen states, which introduces oxygen p character in unoccupied states of mainly metal character. The spectra can be divided into two regions: The first is a double-peaked sharp structure near threshold, which can be related to the metal 3d states; the second is a broader structure 5–10 eV above the edge and is related to the metal 4s and 4p bands. We attribute the oxygen p character up to 15 eV above threshold to mainly oxygen 2p character. The data are analyzed in terms of ligand-field and exchange splittings. It is shown that the splitting between the two sharp peaks near threshold is related closely to the ligand-field splitting, but the relative intensities of the peaks are not fully explained at the present time.

I. INTRODUCTION

In this study we try to learn something about the electronic structure of binary 3d-transition-metal oxides, which still is not well understood despite many past studies.[1–9] By studying the oxygen 1s (or K) absorption edge of binary oxides, we hope to set up a reference for the interpretation of x-ray-absorption edges and the electronic structure of more complex compounds, such as the high-T_c superconducting oxides. The oxygen 1s edge, with an absorption energy of about 530 eV, is situated in the energy range between 300 and 1000 eV, which until recently was technically difficult to reach. The relatively underdeveloped role of this energy region, containing besides the oxygen 1s edge also the 3d–transition-metal 2p (or $L_{2,3}$) edges, compared to, e.g., the transition-metal 1s (or K) edges is predominantly caused by poor monochromator resolution. Studies such as ours, with an instrumental resolution of ~500 meV, are now feasible as a result of the development of new and better monochromators for synchrotron radiation in this energy range.[10]

X-ray absorption (XAS) is a local process in which an electron is promoted to an excited electronic state, which can be coupled to the original core level with the dipole selection rule stating that the change in the angular momentum quantum number (ΔL) is ± 1, while the spin is not changed.[11] For the oxygen 1s edge ($L=0$) this means that only oxygen p character ($L=1$) can be reached. The resulting spectrum can be envisaged in a first-order approximation as an image of the oxygen p projected unoccupied density of states. For more detailed studies, we note below three problems in relating a calculated DOS to an XAS spectrum.

First, the usual way to calculate the density of states is via the Hohenberg-Kohn density-functional theory within the Kohn-Sham local-density approach[12] (LDA). Using the LDA, the occupied part of the DOS calculation is a routine task for the 3d-transition-metal oxides. For the unoccupied states there are, however, purely technical problems of the requirements for more extended basis sets and avoidance of inappropriate linearization schemes.[13] For instance, the O 3p levels, which begin 10–15 eV above E_F, are not included in density-of-states (DOS) calculations with a basis set limited to one wave function per L value. Thus, most published calculations[6–8] are limited to the first few eV of the unoccupied states. Unfortunately, we know of only one oxide band-structure calculation (for CuO) (Ref. 13) whose basis set is sufficient for a sensible comparison with XAS far above threshold. Calculations also exist within the multiple-scattering formalism which treat the unoccupied density of states (UDOS) up to some 50 eV above threshold.[14] However, these calculations, which are used in the description of the transition-metal 1s x-ray-absorption near-edge spectroscopy (XANES) spectra, have not been published for the oxygen 1s edges of many of the oxides we consider here. A second technical problem concerns the single-particle matrix elements for XAS.[15] Here we will assume that the oxygen $1s \rightarrow np$ matrix elements are constant for any given n unless otherwise stated.

Finally, there is an important problem of principle. Even if the UDOS was calculated correctly within LDA and corrected for single-particle matrix elements,[15] a comparison to the x-ray-absorption edges is not strictly valid. The excited electron in the final state interacts with its surroundings, modifying the density of states due

to correlation. Moreover, the created core hole affects the final-state DOS, as has, for instance, been shown for the early-transition-metal $2p$ ($L_{2,3}$) (Ref. 16) and Al and Si $1s$ (Ref. 17) x-ray-absorption spectra. Both effects come under the heading of self-energy. For the oxygen $1s$ edges these effects probably are less severe, compared to the transition-metal $2p$ edges, because the core hole now is situated on oxygen while the states in the unoccupied bands just above the Fermi level have most weight on the metal sites. Oxygen $2p$ character hybridizes with these unoccupied metal bands, but the $1s$ hole on oxygen only indirectly influences them.

Because not much high-resolution data are available, and even more because of the lack of suitable calculations of the UDOS, we confine ourselves here to a more empirical approach as a starting point. In this paper we study a series of $3d$-transition-metal oxides, of which all but one (CuO) contain a transition metal which is octahedrally surrounded by oxygen. The major variation is the number of $3d$ electrons, ranging from zero to nine. Also the formal valency varies between 2 and 4, resulting in different crystal structures for each valency: Sc_2O_3, Ti_2O_3, V_2O_3, Cr_2O_3, and Fe_2O_3, each with the corundum structure; TiO_2, VO_2, and MnO_2, each with the rutile structure and the complex inverse spinel-structures Fe_3O_4. We also consider the spectra of the monoxides TiO, MnO, FeO, NiO, and CuO of Nakai *et al.*[18] The first four materials have the rocksalt structure and CuO has its typical structure in which Cu is surrounded by four oxygen atoms. The measurements on NiO and CuO were repeated by us to check the reproducibility of the results under different experimental conditions. We note that especially the monoxides discussed are defect structures;[19] defects can have a considerable influence on XAS spectra as they distort the local symmetry.[20] Besides the known defect structures of the monoxides, the samples measured as commercial powders (see Sec. II) can be expected to contain a fair amount of defects. As a start we will consider all compounds as stoichiometric; the possible effects of nonstoichiometry are discussed in Sec. IV F.

After a short description of the experimental conditions (Sec. II), we will present the oxygen $1s$ edges. In their interpretation we will focus on the transition-metal $3d$-band region (Sec. III). In the discussion (Sec. IV) a comparison is made with the ligand-field-splitting data from the literature and simple models to explain the specific shapes of the $3d$-band region are discussed.

II. EXPERIMENTAL

The x-ray-absorption measurements were carried out at the Berlin synchrotron-radiation source BESSY, using the SX700 plane-grating monochromator.[10] The contribution to the resolution could be reasonably simulated by a Lorentzian of about 0.5 eV full width at half maximum[21] (FWHM). However, it should be noted that our spectra show as much detail as those of Nakai *et al.*,[18] who claims 0.1 eV monochromator resolution. The spectra were recorded in the total-electron-yield mode. They were normalized to the beam current, to correct for synchrotron-intensity loss during a measurement. The samples used were commercial powders (Sc_2O_3, Ti_2O_3, VO_2, V_2O_3, and Cr_2O_3) and natural minerals (TiO_2, MnO_2, MnO, Fe_2O_3, Fe_3O_4, and NiO). CuO was obtained as a single crystal from Oxford Laboratories. Solid samples were scraped under vacuum to ensure clean surfaces and were thus preferred to powders. The pressure during measurements was in the 10^{-9} torr range.

The throughput of Cu was measured at the oxygen $1s$ edge to check for oxygen contamination in the monochromator. No contamination was found. The energy calibration of the monochromator was performed by taking pure transition metals (V, Cr, Mn, Fe, and Ni) $2p$ edges and using the energy-loss data of Fink *et al.*[16] as a reference. The calibration curve was linear in the energy range probed (400–800 eV). Comparing our numerical results for NiO and CuO with those of Nakai *et al.*[18] showed in both cases that our threshold was shifted 0.3 eV to higher energy, which at this time is an acceptable disagreement for these XAS edges.

III. RESULTS AND INTERPRETATION

Figures 1(a) and 1(b) show the oxygen $1s$ edge x-ray-absorption spectra of a series of $3d$-transition-metal oxides. The spectra have been approximately normalized to the peak heights; absolute normalization of the intensity scale is not feasible. The spectra have strong structure up to at least 15 eV above threshold and it is this structure we wish to interpret. First, we note that the data presented here are in good agreement with the high-resolution data that exist for TiO_2 (Ref. 22) and for NiO and CuO.[18] There is also no disagreement with the available lower-resolution spectra.[23–25] Besides the oxygen $1s$ edge data there are results on the metal edges of $3d$-transition-metal oxides.[26,27] These are significant for a complete picture of the electronic structure. However, in this paper we do not include the discussion of the metal edges and consider only the oxygen $1s$ edge.

We divide the spectra into two regions. The first, shaded in the figures, is attributed to oxygen $2p$ weight in states of predominantly transition-metal $3d$ character: the transition-metal $3d$ band. This assignment conforms with that of Fisher[23] and other studies,[22,28,29] based on a molecular-orbital treatment. Further discussion of this region is given in Sec. IV.

The second region, typically 5–10 eV above threshold, is attributed to oxygen p character hybridized with metal $4s$ and $4p$ states.[30] Detailed calculations on CuO with an extended basis set (with the inclusion of both oxygen $2p$ and $3p$ character) show this to have principally oxygen $2p$ (not $3p$!) character, with the $2p$ count reaching ~ 6 at about 15 eV above E_F.[13] We proceed under the assumption that the peaks up to about 15 eV in the other transition-metal oxides are also due to oxygen $2p$ character in the unoccupied states. This high-energy range of spread for oxygen $2p$ character is an indication of strong covalency in these materials and is not in disagreement with traditional chemical ideas.[31] From Fig. 1 and Table I a common structure of the $4sp$ band, consisting of a main peak (E_{p2}) and a low-energy shoulder (E_{p1}) at approximately 3.2 eV ($=\Delta p$), appears throughout the series.

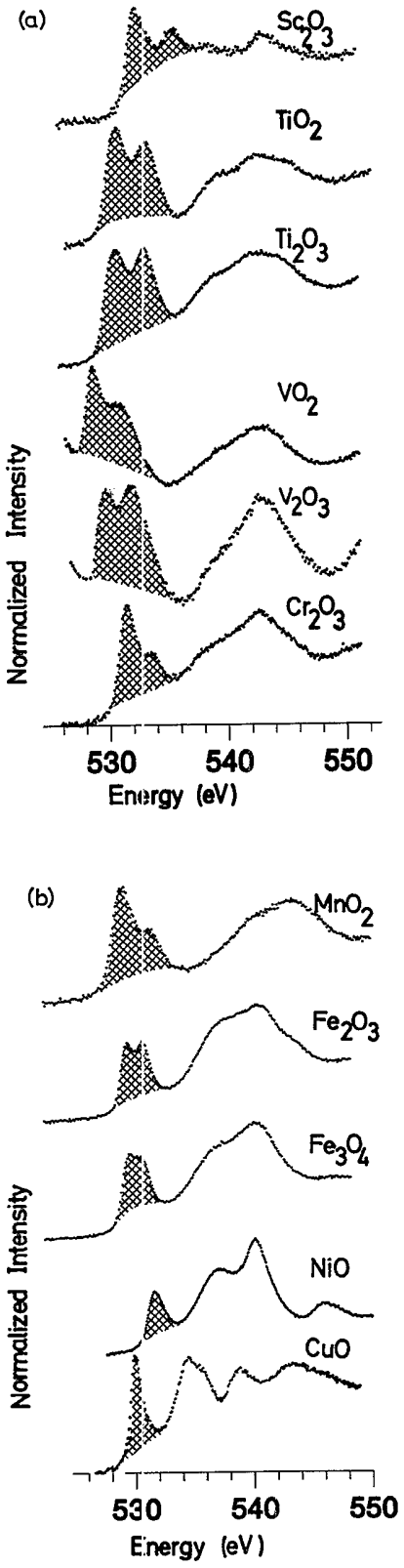

FIG. 1. (a) and (b) Oxygen 1s x-ray-absorption spectra: the shaded area is assigned to oxygen p character in the transition-metal $3d$ band. The broader structure above is assigned to oxygen p character in the metal $4s$ and $4p$ bands. The vanadium edges are distorted by the tail of the vanadium L_2 edge.

This structure can be related to the O_H symmetry set up by the nearest (oxygen) neighbors, which octahedrally surround the $3d$-transition-metal atoms. It shows no strong dependence on the specific crystal structure. This structure is absent in the nonoctahedral CuO.

A salient point is the decrease in intensity of the $3d$ band, relative to the $4sp$ band across the transition-metal series (see Fig. 2). As noted above, the dominant reason for this is the decrease in the number of unoccupied $3d$ states available for mixing with O $2p$ states; this means that the intensity of the XAS spectra should be linear with the number of holes as is indicated by the line in Fig. 2. However, there is a substantial lower intensity of the $3d$-band region, especially for the d^5 and d^6 oxides. This additional loss of intensity can be explained by the diminished hybridization of the metal $3d$ orbitals with the oxygen $2p$ orbitals due to shrinking of the metal $3d$ orbitals in the late-transition-metal oxides. Note that we have plotted the relative intensity of the $3d$ region with respect to the $4sp$ region. The intensity of this latter region also will be influenced by hybridization. We can say something more about the changes in hybridization in the $3d$ and $4s$ bands with the use of the hybridization strengths (Δ values) from Andersen *et al.*[32] For all transition metals they give tables of the Δ values of each individual l band ($l=0,1,2,3$). This Δ value, a potential parameter in the linear muffin-tin orbital (LMTO) calculation, is proportional to the amplitude of the corresponding radial wave function at the average Wigner-Seitz radius of the lattice. The hybridization is equal to $\Delta^{1/2}$, which gives a direct relation between Δ and the intensity of the $3d$ and $4s$ bands. The values for the pure metals give a clear and—except for titanium—monotone trend to smaller $3d$ versus $4s$ hybridization with a higher atomic number. Using these (metal) values for the oxides, we have to multiply the number of holes (the straight line in Fig. 2) by Δ_{3d}/Δ_{4s} and renormalize the plot. We find that the experimental points are scattered around the resulting curve. This indicates strongly that the additional

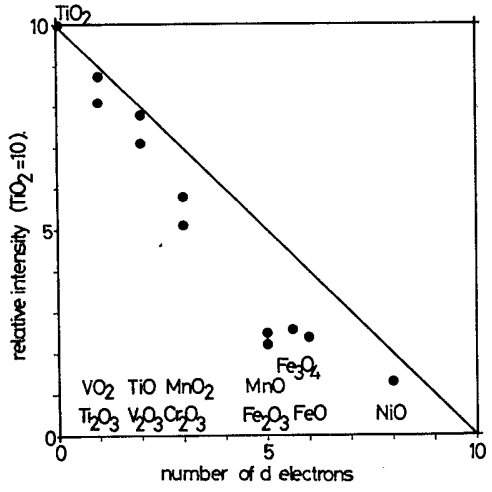

FIG. 2. The intensity of the $3d$-band region with respect to the $4sp$ region is plotted against the number of $3d$ electrons in the ground state. The intensity of TiO_2 is set to 10. The line gives the expected intensity ratio, assuming this is proportional to the number of holes.

loss of intensity can be explained by taking into account hybridization of both the 3*d* and 4*s* bands. (The curve itself is not included in order not to mislead the reader; a complete treatment would involve calculation of the Δ's for the oxides.)

IV. DISCUSSION

A. Implication of the O 1*s* XAS for ideas on covalency

In a purely ionic model, oxygen would have the configuration O $1s^2 2s^2 2p^6$ and the $1s \rightarrow 2p$ channel would be closed in XAS. Covalency reduces the number of filled states with O 2*p* character, so that the strength of the O 1*s* signal at threshold is related to the degree of covalency.[33] It is well known that the transition-metal oxides are not ionic, but have a considerable covalent contribution. There is much evidence for this from pure computations as well as from comparison of computed and experimental magnetic or ligand-field effects.[5,34,35] It is of particular interest that the ligand-field splittings calculated for early-transition-metal oxides in an ionic model (the crystal field) are about a factor of 3 smaller than those found by optical measurements, but come out correctly when covalency is taken into account.[34] The discrepancies are smaller in the late-transition-metal oxides, which is extra evidence that the (oxygen 2*p*–metal 3*d*) hybridization is smaller in the late-transition-metal

TABLE I. (a) The crystal structures, formal valencies, and number of *d* electrons are given. From the spectra in Fig. 1 and from Ref. 19 the first (E_{d1}) and second (E_{d2}) peak positions of the 3*d* band (shaded area) and the first (E_{p1}) and second (E_{p2}) peak positions of the 4*sp* band are measured. (b) The peak splittings and widths of the oxygen 1*s* XAS spectra: the separation of E_{d1} and E_{d2} is identified with the ligand-field splitting (Δ*d*). The characteristic 3.2-eV distance between E_{p1} and E_{p2} in the *sp* band is given as Δ*p*. The left-side HWHM(*l*) of the first peak (Γ_E), the FWHM of the total 3*d* band (Γ_d), and the FWHM of the 4*sp* band (Γ_p) are given. The O 1*s* edges in VO_x are distorted by the tailing effect of the vanadium *L* edges. We estimate the uncertainty in Γ_D as ±0.3 eV. All energies are in eV.

(a)

Compound	Crystal structure	Valency	*d* count	E_{d1}	E_{d2}	E_{p1}	E_{p2}
Sc_2O_3	corundum	3+	0	532.4	535.7		543.1
TiO_2	rutile	4+	0	530.7	533.3	539.4	542.7
Ti_2O_3	corundum	3+	1	530.8	533.2	539.0	542.2
TiO[a]	rocksalt	2+	2	530.2	533.0	539.5	542.5
VO_2	rutile	4+	1	528.8	531.0	540.4	543.1
V_2O_3	corundum	3+	2	529.8	531.9	539.2	542.8
Cr_2O_3	corundum	3+	3	531.4	533.7	538.4	542.7
MnO_2	rutile	4+	3	528.9	531.4	540.5	543.4
MnO[a]	rocksalt	2+	5	529.6	530.9	538.4	542.5
Fe_2O_3	corundum	3+	5	529.4	530.7	537.4	540.6
Fe_3O_4	inverse spinel	2+ and 3+	5 and 6	528.9	530.5	537.1	540.2
FeO[a]	rocksalt	2+	6	529.8	531.0	536.3	540.2
NiO	rocksalt	2+	8		531.7	537.0	540.2
NiO[a]	rocksalt	2+	8		531.4	536.7	540.0
CuO	CuO	2+	9		530.1	534.6	535.9
CuO[a]	CuO	2+	9		529.8	534.3	535.6

(b)

Compound	Γ_E HWHM(*l*)	Γ_D FWHM	Γ_P FWHM	Δ*d*	Δ*p*
Sc_2O_3	0.8	6.0		3.3	
TiO_2	1.0	4.8	9.5	2.6	3.3
Ti_2O_3	1.2	5.3	9.1	2.4	3.2
TiO[a]	0.6	5.3	9.1	2.8	3.0
VO_2	0.9	4.9	7.6	2.2	2.7
V_2O_3	1.0	4.9	6.5	2.2	3.6
Cr_2O_3	0.9	3.6	7.3	2.3	4.3
MnO_2	0.9	4.2	8.5	2.5	2.9
MnO[a]	0.6	3.7	7.8	1.3	4.1
Fe_2O_3	0.7	3.3	8.4	1.3	3.2
Fe_3O_4	0.8	3.0	7.1	0.9	3.1
FeO[a]		3.8	6.8	1.2	3.3
NiO	0.7	2.3	6.7		3.2
NiO[a]	0.6	2.0	5.6		3.3
CuO	0.6	1.4	3.2		1.3
CuO[a]	0.45	1.1	3.3		1.3

[a]Data taken from Reference 19.

oxides, as we already suggested in the discussion of the intensities of the 3*d* band throughout the series.

Because of the technical problems in computing the unoccupied DOS over some energy range, it is not always realized that there is considerable weight of O 2*p* character in states 10–15 eV above E_F. The evidence from the LASW calculation of CuO is that most O *p* character up to 15 eV above E_F is in fact O 2*p*.[13] The O 1*s* XAS spectra of the transition-metal oxides show similar broad peaks, which we have attributed to O 2*p* character in bands with predominantly transition-metal 4*sp* character. We note that the integrated intensity of the broad 4*sp* band is comparable to that of the 3*d* band. In the very reasonable first approximation of constant O $1s \rightarrow 2p$ matrix elements, the XAS intensity is proportional to the weight of O 2*p* character in a band. Thus, in chemical language, the observed intensity ratios in the two spectral regions is evidence that, besides the metal 3*d* states, also the metal 4*sp* states are important for the covalency of transition-metal oxides.

B. Ligand-field splittings

We now examine more closely the first structure, the 3*d* band, which is shaded in Fig. 1. This structure consists of two (often similar) peaks. In a first approximation these two peaks can be identified as the t_{2g}- and e_g-symmetry bands separated by a ligand-field splitting; we shall use the term "ligand-field splitting" to denote the "bare" (ionic) crystal-field splitting plus hybridization.[36]

To check the validity of the assignment of the two sharp peaks as being related to the t_{2g} and e_g symmetry, with the peak separation mirroring the ligand-field splitting, we first compare our splittings, Δd, with optical data of octahedrally hydrated transition-metal ions, which have been related to the ligand-field splitting.[5,37] In this comparison some precautions must be taken. Obviously the materials compared are not identical, though in both cases the transition metal is octahedrally surrounded by oxygen ions. Bearing this in mind we compare the results for the ligand-field splitting which are tabulated in Table II. Considering the precision in the determination of our Δd value, good agreement is found for all five transition-metal oxides.

In contrast to the "general rule" that the ligand-field splitting of trivalent ions is around 2.5 eV and the divalent-ion ligand-field splitting is approximately half that value,[5] we come to the generalization of the division of early- and late-transition-metal oxides, the early-transition-metal oxides with a splitting around 2.5 eV and the late-transition-metal oxides with a splitting round 1.2 eV, as can be checked in Table I. The dividing line between early- and late-transition-metal oxides is the presence of a filled e_g orbital in the ground state. Up to d^3 compounds only t_{2g} states are filled. From d^5 compounds the filled e_g states increase the lattice parameter with respect to the orbital radii, which decrease throughout the 3*d*-transition-metal series. The consequence for the 3*d* orbitals is a decrease of hybridization as we discussed in Sec. III. The d^4 compounds fall in between the early- and late-transition-metal compounds.

TABLE II. Comparison of the splitting between the t_{2g} and e_g peak in XAS (Δd), with optical data of the ligand-field splitting (LFS) in hydrated transition-metal ions (Ref. 6).

Compound	Δd	LFS
Ti_2O_3	2.4	2.5
V_2O_3	2.2	2.2
Cr_2O_3	2.3	2.1
MnO	1.3	1.5
Fe_2O_3	1.3	1.6

Despite the "disagreement" in the generalizations made, the good individual correspondences of Δd with the optical ligand-field-splitting data give us confidence that the splitting between the two peaks in the 3*d* band is the same as that attributed to the ligand-field splitting in optical spectra.

C. The intensities of the so-called t_{2g} and e_g peaks

XAS data on peak splittings are analogous to those given by optical-absorption spectroscopy, except that XAS can more easily be used for d^0 materials. However, oxygen 1*s* XAS spectra also contain information on the peak intensity ratios, which have no analogy in optical data, and in fact our analysis of these intensities will indicate a serious problem, and possibly the need to revise the assignment somewhat. We will develop the ideas of the peak intensities step by step.

The simplest and first effect to be taken into account is the electron counting. The t_{2g} orbitals (*xy*, *xz*, and *yz*) can take six electrons and the e_g orbitals (x^2-y^2, z^2) can take four. Thus the ratio of empty orbitals t_{2g}:e_g is 6:4 for d^0 compounds and decreases to zero in low-spin compounds as the electron count is increased to d^6. This is shown by the dashed line in Fig. 3. However, note that for high-spin materials the exchange splitting may lead to filling of the majority-spin e_g states before the minority-spin t_{2g} states. Thus for high-spin compounds the ratio of t_{2g}:e_g holes rises from 3:4 at d^3 to 3:2 at d^5, before dropping to 0:2 at d^8, as is shown by the upper dashed line in Fig. 3. The curves based on electron counting in Fig. 3 may be compared with the experimental ratio of the first to second peaks. Although the separation of the two peak areas is only approximate, we immediately see some serious discrepancies. There is considerable scatter of the experimental points, which may be an indication of the accuracy of the separation, but for the d^3 materials Cr_2O_3 and MnO_2 the ratio of the low-energy to the high-energy peak is much too high to be explained by ideas based on electron counting.

D. Orbital hybridization

We note that even where the peak intensity ratio is in reasonable agreement with the electron-count curve, this creates a problem because of the role of orbital hybridization. In octahedral complexes the metal e_g orbitals are directed towards the oxygen atoms and have a stronger overlap with the oxygen 2*p* orbitals. In general it is assumed[1] (following calculations[6,38,39]) that the hybridiza-

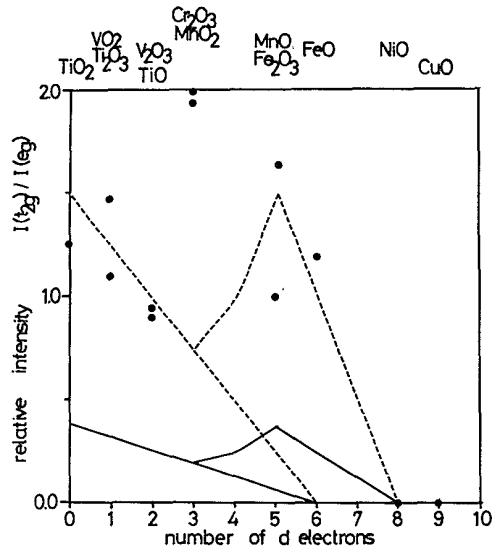

FIG. 3. The relative intensity of the t_{2g} vs the e_g peak is given. The theoretical assumption that the t_{2g} hybridization is half that of e_g hybridization is given as the solid line; the dashed line gives just the electron counting (equal or no hybridization). For the late-transition-metal oxides two lines are given: high-spin states are given with the upper lines; low-spin states with the lower lines. The points are the experimental values (Sc_2O_3 is omitted), which cannot be determined very precisely. For further details, see text.

tion of t_{2g} orbitals (forming π bonds) is about half that of e_g orbitals (forming σ bonds). The ground state of the early-3d-transition-metal compounds can be described by $|t_{2g}^N\rangle+(n_t)^{1/2}\alpha_t|t_{2g}^{N+1}L\rangle+(n_e)^{1/2}\alpha_e|t_{2g}^N e_g L\rangle$, with N ranging from 0 to 3. In the presence of the dominating octahedral surrounding the two distinct states, $|t_{2g}^{N+1}L\rangle$ and $|t_{2g}^N e_g L\rangle$ have to be considered. This implies that due to covalency the d^N state mixed with states in which an electron has jumped from the ligand (in this case a hole of oxygen 2p character is formed) to a transition-metal 3d orbital. This means that as the mixing coefficients α_t and α_e account for the amounts of hybridization with, respectively, t_{2g} and e_g character, $\alpha_t=\frac{1}{2}\alpha_e$.

In oxygen 1s absorption, an electron is excited from the oxygen 1s core state to states with some oxygen p character, i.e., $|t_{2g}^N e_g L\rangle$. Thus we can now relate the intensities to the covalency: $n_t\alpha_t^2$ gives the amount of $|t_{2g}^{N+1}L\rangle$ character in the ground state and it is this character which is probed in the oxygen 1s absorption process. From this it is clear that the intensity ratio I_t/I_e should be equivalent to the amount of covalent mixing $n_t\alpha_t^2/n_e\alpha_e^2=n_t/4n_e$. In Fig. 3 we have compared this ratio (solid line) to the experimental values. It is directly evident that the theoretical lines strongly *underestimate* the experimental ratio, i.e., the relative t_{2g} intensity. At this moment we cannot explain the relative intensities generally observed, despite consideration of several subsidiary effects described below.

E. Exchange splitting

The whole concept of high-spin and low-spin configurations for 3d-transition-metal oxides implies that we must consider exchange effects, which split the two groups of bands, t_{2g} and e_g, into four: spin-up t_{2g}, spin-up e_g, spin-down t_{2g}, and spin-down e_g. Consider, for example, the d^3 compounds Cr_2O_3 and MnO_2, which show a sharp peak near threshold followed by a weak shoulder at 2.4 eV. This result can only be explained if exchange is included. The exchange splitting is proportional to the number of unpaired spins, being three in d^3 compounds. For Cr^{3+} the tabulated exchange splitting per spin is about 0.9 eV.[40] The total splitting becomes 2.7 eV, which is about the same value as the ligand-field splitting (=2.3 eV). Including this exchange splitting makes the approach to the spectrum quite different. Looking at the spectrum (see also Fig. 4), the first peak can be assigned to a superposition of the spin-down t_{2g} state and the spin-up e_g state with a total number of five electrons. The second peak (shoulder) relates to the remaining two spin-down e_g electrons. This superposition is thus a consequence of the equivalent values of exchange and ligand-field splitting.

The result of including exchange effects here is that the electron-counting method increases the peak ratio to 5(3+2):2. If hybridization is included with a factor of 2, as in Sec. IV D, this value is still only decreased to $(\frac{3}{4}+2):2=1.7$. It is clear that a value of the t_{2g}:e_g hybridization ratio could be chosen so as to fit the experimentally observed peak ratio. We conclude on the basis of this analysis for d^3 compounds that exchange effects should not be ignored. However, there are other compounds with other numbers of d electrons for which exchange splittings cannot explain the discrepancies in Fig. 3. An example are the high-spin d^5 compounds MnO and Fe_2O_3

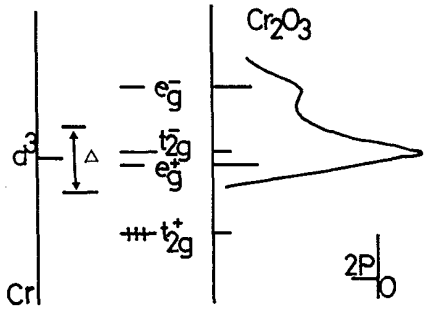

FIG. 4. The line spectrum for d^3 Cr_2O_3 is given. First, a single energy level is given. This level is split by the crystal-field splitting (Δ=2.3 eV) into a t_{2g} (six electrons) and an e_g (four electrons) level. Then the exchange splitting of about 2.7 eV is considered. The result is that the e_g spin-up and t_{2g} spin-down levels almost coincide. The t_{2g} spin-up level is filled with three electrons; this leaves the other three levels empty, and thus they are candidates for absorption. The fourth series of lines gives the amount of oxygen 2p character which is hybridized with the metal 3d states (in fact, the square is given). The assumption that e_g hybridizes twice as much as t_{2g} (and consequently that the intensity is 4 times as much) is used. The heights of these lines should be reflected in the XAS spectra. In Fig. 5 we will use the same way of presenting the energy levels.

for which the energy levels are illustrated in Fig. 5. The exchange splitting is much larger than the crystal-field splitting, so that spin-up t_{2g} and e_g states are filled and the spin-down ones are empty. As a consequence, the exchange splitting does not change the ratio of the two peaks and the intensity ratio t_{2g}:e_g should be $\frac{3}{4}$:2=0.38 when the different hybridization is taken into account. This is far lower than the values measured (1.0 and 1.6).

F. Possible reasons for the discrepancies

In the solid, bond formation leads to broadening of the t_{2g} and e_g levels. It is probable that the t_{2g} and e_g descriptions are only approximately applicable to the two peaks observed and to some extent t_{2g} and e_g character is spread throughout the whole region of the unoccupied 3*d* levels.[41] This will modify the spectra distributions directly. In addition, it opens the possibility for the core-hole potential to shift weight towards the threshold. We have argued earlier that the influence of the core hole on the oxygen 1*s* site is small because the unoccupied states have principally metal 3*d* character. However, this does not mean it can be ignored completely in the context of intensity distributions within the rather narrow, empty 3*d* region. There may be other reasons for the anomalous intensity ratios we find, but we feel that these two effects of band formation cannot be dismissed without further quantitative investigation.

A further reason of discrepancies might be found in the nonstoichiometry of some samples; defects distort the local symmetry and lead to some variation in the interatomic distances. This results in a variation in the amount of hybridization,[42] which in principle can influence the t_{2g} versus e_g intensity distribution and also the ligand-field splitting. We note that although computed charges of the vanadium 1*s* XAS spectra from $VO_{0.8}$ to $VO_{1.25}$ are quite large,[20] published vanadium 1*s* spectra show a smaller sensitivity, which, if reproduced at the oxygen 1*s* edges, would not be large enough to explain the discrepancies we observe. Although we have not considered defects in detail here, we have measured NiO in its black (defect-rich) and green form.[43] Their oxygen 1*s* XAS spectra were identical, which suggests that defects are not too critical for the shape of the spectra. A study of Li-doped NiO (or $Ni_{1-x}Li_xO$) which results in oxygen 2*p* holes,[44] revealed that besides the extra peak at the edge (2*p* hole states) the rest of the spectrum did not change much, except for an increasing width of the peaks. This may not be true for highly defective oxides, like VO and TiO, and the question of the influence of defects deserves much more detailed study. However, the results discussed in this paragraph suggest that defects cannot explain the discrepancies we discuss.

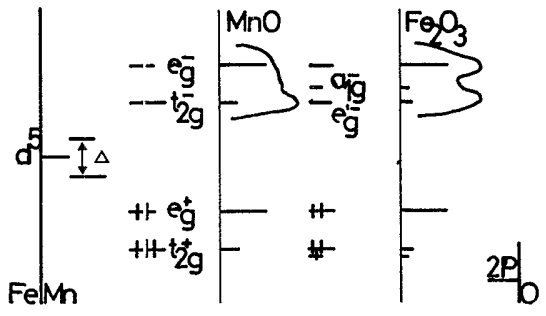

FIG. 5. The line spectra for d^5 MnO and d^5 Fe_2O_3 are given. The exchange splitting of five electrons is much larger than the ligand-field effects. This leaves only the spin-down levels empty. The symmetry of Fe_2O_3 is broken and as a consequence the t_{2g} level is split. The given splitting is not quantitative. The decrease of the Fe_2O_3 t_{2g} peak (compared to MnO) can be related to this broken symmetry.

V. CONCLUDING REMARKS

All oxygen 1*s* absorption edges of the transition-metal oxides can be divided into two regions. In the first, near threshold, the oxygen 2*p* character is hybridized with the sharp structured transition-metal 3*d* band. In the second region, O 2*p* character is hybridized with the weakly structured 4*sp* band. The integrated intensity of the 4*sp* region is at least equal to the 3*d*-band region, which indicates that the metal 4*sp* states are important for the covalency of the transition-metal oxides. The metal 4*sp* hybridization gives a more or less constant bonding effect above which the metal 3*d* hybridization accounts for the specific, material-dependent, effects.

The 3*d* band consists of two peaks, which we believe are mainly related to, respectively, t_{2g} and e_g symmetry, despite the observation of anomalous intensity ratios. For all oxides considered, the ligand-field-splitting parameter, from optical spectroscopy, is well reproduced by the separation of the first two sharp XAS peaks. for Cr_2O_3 and MnO_2 the description of the combined effect of ligand-field and exchange splitting leads to the conclusion that the first peak is an "accidental" superposition of t_{2g} spin-down and e_g spin-up states, while the second peak relates to the remaining e_g spin-down states.

The intensities of t_{2g} and e_g do not conform with the rule that e_g hybridization is twice as big at t_{2g} hybridization.[1,6] Across the series the intensity of the t_{2g} peak is underestimated. The reason is not clear to us, but we believe that band formation in the solid, with all its consequences, may explain at least some of the discrepancies.

Our analysis showed that an important factor determining the shape and magnitude of the 3*d* region in the oxygen 1*s* XAS spectra of the 3*d*-transition-metal oxides is the presence of a filled e_g orbital in the ground state. This criterion splits the 3*d*-transition-metal oxides into two main groups: the early- (or light) 3*d*-transition-metal oxides with zero to three *d* electrons, and the late- (or heavy) 3*d*-transition-metal oxides with five or more *d* electrons, which are more localized.

ACKNOWLEDGMENTS

We thank S. Hüfner for constructive discussions, W. Braun for his efforts in coordinating our experiments, and B. E. Watts for provision of a single crystal of CuO. We are grateful to the staff of the Berliner Elektronen Speicherring-Gesellschaft für Synchrotronstrahlung

(BESSY) for their support. This work was supported, in part, by the Dutch Foundation for Chemical Research [Stichting Scheikundig Onderzoek Nederland (SON)] with financial assistance of the Netherlands Organization for Scientific Research [Nederlandse Organisatie voor Wetenschappelijk Onderzoek (NWO)] and by the Committee for the European Development of Science and Technology (CODEST) program.

[1]G. A. Sawatzky, in *Narrow Band Phenomena,* edited by J. C. Fuggle, G. A. Sawatzky, and J. W. Allen (Plenum, New York, 1988).

[2]J. B. Goodenough, Phys. Rev. **117**, 1442 (1960); Prog. Solid State Chem. **5**, 145 (1972).

[3]J. B. Goodenough, in *Magnetism and the Chemical Bond* (Wiley-Interscience, New York, 1963).

[4]P. W. Anderson, Phys. Rev. **115**, 2 (1959).

[5]S. Sugano, Y. Tanabe, and H. Kitamura, in *Multiplets of Transition Metal Ions in Crystals* (Academic, New York, 1970).

[6]L. F. Mattheiss, Phys. Rev. **5**, 290 (1972); **5**, 306 (1972).

[7]J.-L. Calais, Adv. Phys. **26**, 847 (1977).

[8]A. Neckel, P. Rastl, R. Eibler, P. Weinberger, and K. Schwarz, J. Phys. C **9**, 579 (1976).

[9]K. Terakura, T. Oguchi, A. R. Williams, and J. Kübler, Phys. Rev. B **30**, 4734 (1984).

[10]Examples of high-resolution monochromators for the oxygen 1*s* edge (500 eV) are the SX700 at BESSY, Berlin, H. Petersen, Nucl. Instrum. Methods A **246**, 260 (1986); the 10-m grazing-incidence monochromator at the Photon Factory, H. Maezawa, S. Nakai, S. Mitani, A. Mikuni, T. Namioka, and T. Sasaki, Nucl. Instrum. Methods A **246**, 310 (1986); and the Dragon monochromator at Brookhaven National Laboratory, C.T. Chen, Nucl. Instrum. Methods A **256**, 595 (1987). The pace of development in this area is so high that within the last year 500 meV resolution can be significantly bettered in some instruments.

[11]For example, R. D. Cowan, in *The Theory of Atomic Structure and Spectra* (University of California Press, Berkeley, 1981).

[12]For example, L. Hedin, Phys. Rev. **139**, A796 (1965).

[13]We know of only one oxide band-structure calculation (for CuO), whose basis set includes also the metal 4*s* and 4*p* and the oxygen 3*s* and 3*p* states and thus is more appropriate for a comparison with oxygen 1*s* XAS. A detailed comparison for CuO is given by M. Grioni, M. T. Czyzyk, F. M. F. de Groot, J. C. Fuggle, and B. E. Watts, Phys. Rev. B **39**, 4886 (1989); The theoretical and mathematical details concerning this extended basis set are discussed by M. T. Czycyk and R. A. de Groot (unpublished).

[14]D. Norman, K. B. Garg, and P. J. Durham, Solid State Commun. **56**, 895 (1985).

[15]H. Winter, P. J. Durham, and G. M. Stocks, J. Phys. F **14**, 1047 (1984).

[16]J. Zaanen, G. A. Sawatzky, J. Fink, W. Speier, and J. C. Fuggle, Phys. Rev. **32**, 4905 (1985); J. Fink, Th. Müller-Heinzerling, B. Scheerer, W. Speier, F. U. Hillebrecht, J. C. Fuggle, J. Zaanen, and G. A. Sawatzky, *ibid.* **32**, 4899 (1985).

[17]S. W. Kortboyer, M. Grioni, W. Speier, R. Zeller, L. M. Watson, M. T. Gibson, F. Schäfers, and J. C. Fuggle, J. Phys. C (to be published).

[18]S. Nakai, T. Mitsuishi, H. Sugawara, H. Maezawa, T. Matsukawa, S. Mitani, K. Yamasaki, and T. Fujikawa, Phys. Rev. B **36**, 9241 (1987).

[19]A. F. Wells, in *Structural Inorganic Chemistry,* 3rd ed. (Clarendon, Oxford, 1962), p. 475.

[20]F. W. Kutzler and D. E. Ellis, Phys. Rev. B **29**, 6890 (1984).

[21]S. W. Kortboyer, J. B. Goedkoop, F. M. F. de Groot, M. Grioni, J. C. Fuggle, and H. Petersen, Nucl. Instrum. Methods A **275**, 435 (1989).

[22]R. Brydson, B. G. Williams, W. Engel, H. Sauer, E. Zeitler, and J. M. Thomas, Solid State Commun. **64**, 609 (1987).

[23]L. A. Grunes, R. D. Leapman, C. N. Wilker, R. Hoffman, and A. B. Kunz, Phys. Rev. B **25**, 7157 (1982).

[24]D. W. Fisher, J. Phys. Chem. Solids **32**, 2455 (1971).

[25]I. Davoli, A. Macelli, A. Bianconi, M. Tomellini, and M. Fanfoni, Phys. Rev. B **33**, 2979 (1986); G. E. Brown, Jr., G. A. Waychunas, J. Stöhr, and F. Sette, J. Phys. (Paris) Colloq. **47**, C8-685 (1986).

[26]A discussion on TM oxide metal *K* edges is given in A. Balzarotti, F. Comin, L. Incoccia, M. Piacenti, S. Mobilio, and A. Savoia, Solid State Commun. **35**, 145 (1980) (on TiO_2); M. Belli, A. Scafati, A. Bianconi, S. Mobilio, L. Palladino, A. Reale, and E. Burratini, *ibid.* **35**, 355 (1980) (on manganese); A. Bianconi, Phys. Rev. B **26**, 2741 (1982) (on VO_2); G. S. Knapp, B. W. Veal, H. K. Pan, and T. Klippert, Solid State Commun. **44**, 1343 (1982); L. A. Grunes, Phys. Rev. B **27**, 2111 (1983); J. Wong, F. W. Lytle, R. P. Messmer, and D. H. Maylotte, *ibid.* **30**, 5596 (1984) (on vanadium); Th. Lindner, H. Sauer, W. Engel, and K. Kambe, *ibid.* **33**, 22 (1986) (on MgO); S.-H. Chou, J. Guo, and D. E. Ellis, *ibid.* **34**, 12 (1986) (on FeO).

[27]Results on the TM oxide metal $L_{2,3}$ edges can be found in R. D. Leapman, L. A. Grunes, and P. L. Fejes, Phys. Rev. B **26**, 614 (1982); S. L. Hulbert, B. A. Bunker, F. C. Brown, and P. Pianetta, *ibid.* **30**, 2120 (1984) (on Cu_2O).

[28]K. Tsutsumi, O. Aita, and K. Ichikawa, Phys. Rev. B **15**, 4638 (1977).

[29]C. Sugiura, M. Kitamura, and S. Muramatsu, J. Chem. Phys. **84**, 4824 (1986); C. Sugiura, M. Kitamura, and S. Muramatsu, *ibid.* **85**, 5269 (1986); C. Sugiura, M. Kitamura, and S. Muramatsu, Phys. Status Solidi B **135**, K57 (1986); C. Sugiura, M. Kitamura, and S. Muramatsu, *ibid.* **141**, K173 (1987); M. Kitamura, S. Muramatsu, and C. Sugiura, Phys. Rev. B **33**, 5294 (1986); Y. Ohno, K. Hirama, S. Nakai, C. Sugiura, and S. Okada, *ibid.* **27**, 3811 (1983); Y. Ohno and S. Nakai, J. Phys. Soc. Jpn. **54**, 3591 (1985); S. Nakai, K. Ogata, M. Ohashi, C. Sugiura, T. Mitsuishi, and H. Maezawa, *ibid.* **54**, 4034 (1985); S. Nakai, A. Kawata, M. Ohashi, M. Kitamura, C. Sugiura, T. Mitsuishi, and H. Maezawa, Phys. Rev. B **37**,10 895 (1988).

[30]This assignment does agree with, e.g., P. R. Sarode, J. Phys. F **17**, 1605 (1987).

[31]K. Fajans and G. Joos, Z. Phys. **23**, 1 (1923); K. Fajans, Naturwissenschaften **11**, 165 (1923); Z. Krystallogr. **61**, 18 (1924).

[32]O. K. Andersen, O. Jepsen, and D. Glötzel, in *Highlights in Condensed Matter Theory,* edited by F. Bassani, F. Fumi, and M. P. Tosi (North-Holland, Amsterdam, 1985), pp. 82 and 113.

M. P. Tosi (North-Holland, Amsterdam, 1985), pp. 82 and 113.

[33]M. Pedio, J. C. Fuggle, J. Somers, E. Umbach, J. Haase, Th. Lindner, U. Höfer, M. Grioni, F. M. F. de Groot, B. Hillert, L. Becker, and A. Robinson, Phys. Rev. B (unpublished).

[34]J. Owens and J. H. M. Thornley, Rep. Prog. Phys. **29**, 675 (1966); K. W. H. Stevens and C. A. Bates, in *Magnetic Oxides,* edited by D. J. Craik (Wiley, London, 1975), pp. 141ff; A. S. Chakravarty, *Introduction to the Magnetic Properties of Solids* (Wiley, New York, 1980), pp. 271ff, and references therein.

[35]See, e.g., M. Tsukada, J. Phys. Soc. Jpn. **49**, 1183 (1980); M. Tsukada, H. Adachi, and C. Satoko, Prog. Surf. Sci. **14**, 113 (1983).

[36]C. J. Ballhausen, in *An Introduction to Ligand Field Theory* (McGraw-Hill, New York, 1962).

[37]O. W. Holmes and D. S. McClure, J. Chem. Phys. **26**, 1686 (1957).

[38]W. Harrison, in *Electronic Structure and Properties of Solids* (Freeman, San Francisco, 1980).

[39]O. Gunnarsson, O. K. Andersen, O. Jepsen, and J. Zaanen, Phys. Rev. B **39**, 1708 (1989).

[40]C. E. Moore, *Atomic Energy Levels,* Nat. Bur. Stand. (U.S.) Circ. No. 467 (U.S. GPO, Washington, D.C., 1958), Pts. I–III.

[41]This is reflected in a band-structure calculation of TiO_2, as given by S. Munnix and M. Schmeits, Phys. Rev. B **30**, 2202 (1984).

[42]K. E. Smith and V. E. Henrich, Phys. Rev. B **38**, 5965 (1988).

[43]See, e.g., P. A. Cox, in *The Electronic Structure and Chemistry of Solids* (Oxford University Press, London, 1987), pp. 215ff.

[44]P. Kuiper, G. Kruizinga, J. Ghijsen, G. A. Sawatzky, and H. Verweij, Phys. Rev. Lett. **62**, 221 (1989).